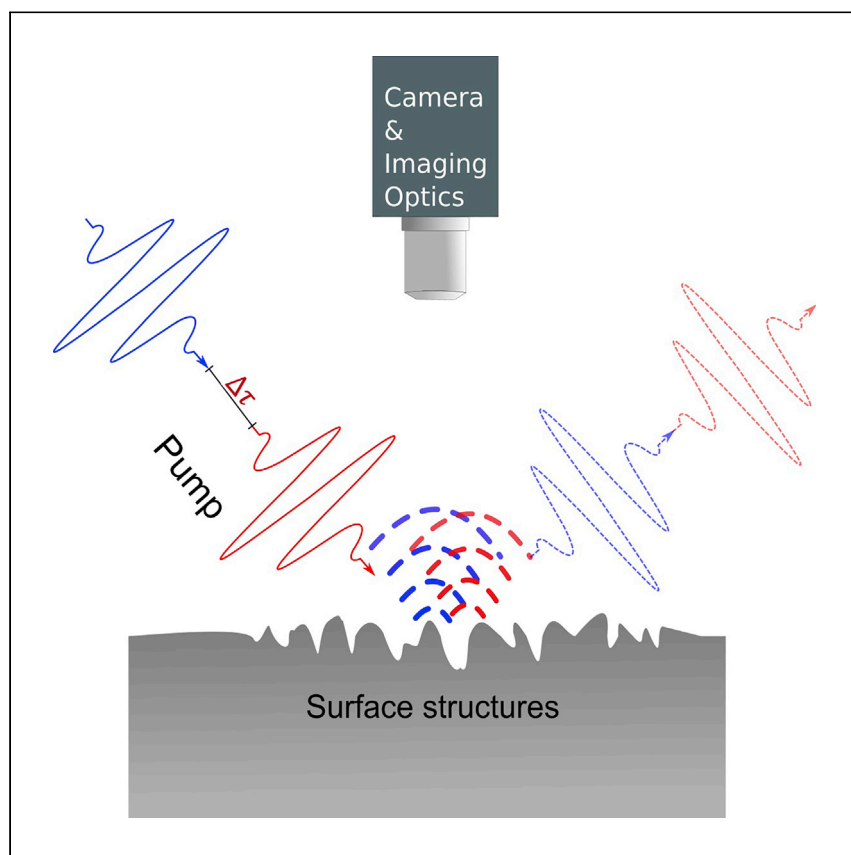


Report

# Imaging nanostructure phase transition through ultrafast far-field optical ultramicroscopy



Ultrafast imaging of nanostructures is challenging due to their low signal-to-noise-ratio. ElKabbash et al. use ultrafast ultramicroscopy to image light-matter interactions at the nanoscale, spatial, and femtosecond scale temporally. The results show that irradiating surface nanostructures with an intense femtosecond laser pulse undergo photomechanical spallation within a few picoseconds.

Mohamed ElKabbash, Ranran Fang, Anatoliy Vorobyev, ..., Billy Lam, Subhash Singh, Chunlei Guo

guo@optics.rochester.edu

### Highlights

Introducing an optical far-field ultrafast imaging method for nanostructures

Imaging photomechanical spallation of nanostructures within picoseconds

Imaging the re-solidification dynamics of nanostructures

## Report

## Imaging nanostructure phase transition through ultrafast far-field optical ultramicroscopy

Mohamed ElKabbash,<sup>1,2</sup> Ranran Fang,<sup>1,2</sup> Anatoliy Vorobyev,<sup>1</sup> Sohail A. Jalil,<sup>1</sup> Sandeep Chamoli,<sup>1</sup> Billy Lam,<sup>1</sup> Subhash Singh,<sup>1</sup> and Chunlei Guo<sup>1,3,\*</sup>

## SUMMARY

Imaging photo-induced ultrafast dynamics of nanostructure phase transition is of great interest to the fields of laser-matter interactions and nanotechnology. However, conventional ultrafast far-field optical imaging methods cannot image nanostructures as their scattering scales as  $D^6$ , with  $D$  being the diameter, leading to a vanishing signal-to-noise ratio. Here, we use ultrafast ultramicroscopy to capture the spatiotemporal evolution of surface nanostructures as they undergo melting, spallation, and re-solidification processes. Our experimental observations, combined with finite difference time domain (FDTD) simulations, show agreement with molecular dynamic simulations on ultrashort laser pulse-irradiated metallic nanoparticles and suggest the occurrence of melting of nanostructures followed by photomechanical spallation within a few picoseconds. At longer timescales, we image the re-solidification dynamics of the melted nanostructures occurring within nanoseconds. The re-solidification time for nanostructured surface occurs an order of magnitude faster than for an initially flat surface. Our study demonstrates a simple but powerful far-field optical approach for studying ultrafast dynamics of nanostructures.

## INTRODUCTION

Surface nanostructures play a crucial role in modifying the surface optical, electrical, mechanical, chemical, and wetting properties of materials.<sup>1,2</sup> Direct femtosecond (fs) laser nanostructuring enabled a range of technological advancements including highly floatable metallic assemblies,<sup>3</sup> enhanced solar absorption of Si photovoltaic cells,<sup>4</sup> selective solar absorbers,<sup>5</sup> and high-efficiency solar water purification.<sup>6</sup> Past studies postulated the physical mechanisms behind the formation of different types of nanostructures through fs laser processing by inspecting the final scanning electron microscopy (SEM) images of the laser-ablated surfaces.<sup>7</sup>

On the other hand, molecular dynamics (MD) simulations revealed several mechanisms responsible for material removal in laser ablation and processing, e.g., coulomb explosion and photomechanical spallation<sup>8,9</sup> In particular, MD simulations were recently used to study the photo-induced dynamics of metallic nanoparticles irradiated with ultrashort optical pulses.<sup>10,11</sup> For sufficiently intense and short laser pulses, the nanoparticle temperature far exceeds the critical melting and boiling temperatures, i.e., the nanoparticle is highly superheated. The superheated nanoparticle undergoes rapid melting and experiences compressive pressure, and a rarefaction wave propagates toward its center. This process results in two

<sup>1</sup>The Institute of Optics, University of Rochester, Rochester, NY 14627, USA

<sup>2</sup>These authors contributed equally

<sup>3</sup>Lead contact

\*Correspondence: [guo@optics.rochester.edu](mailto:guo@optics.rochester.edu)  
<https://doi.org/10.1016/j.xcrp.2021.100651>



counter-propagating rarefaction waves creating tensile stress inside the nanoparticle.<sup>11</sup> The tensile pressure creates voids that subsequently lead to spallation of the nanoparticles that fragments into clusters of smaller particles.

Experimentally, imaging the photo-induced ultrafast dynamics of nanostructures was demonstrated using ultrafast variants of high spatial resolution imaging methods, e.g., fs X-ray diffraction imaging and ultrafast electron microscopy (UEM). Although fs X-ray diffraction imaging provides a high spatial and temporal resolution, it requires extensive image reconstruction algorithms that is challenging for delay times >1 ns.<sup>12,13</sup> Moreover, the intensity of the X-ray probe is often higher than the damage threshold of imaged materials, making it impossible to determine the re-solidification dynamics.<sup>13</sup> UEM requires vacuum operation with highly specialized instrumentation and is not suitable for materials resistant to electron beams.<sup>14–16</sup> Optical far-field ultrafast imaging of nanostructures that is necessary to validate MD theoretical predictions, however, remains challenging. To overcome these challenges, we introduced a dark-field ultrafast imaging approach (ultrafast ultramicroscopy) that we used to image the formation of surface structures after ablating a smooth surface.<sup>17</sup> However, ultrafast ultramicroscopy has not been used to image the photo-induced dynamics of nanostructures.

Here, we study the non-repetitive ultrafast photo-induced dynamics of nanostructures using ultrafast ultramicroscopy. We demonstrate the ability of the ultrafast ultramicroscopy approach to collect scattered light from nanostructures even for a highly reflecting substrate. We directly image Zn surface nanostructures as they go through the entire melting, spallation, and re-solidification processes following laser irradiation. By combining our imaging method with finite difference time domain (FDTD) simulations and image correlation analysis, our results suggest the occurrence of rapid melting followed by photomechanical spallation of the nanoparticles within a few picoseconds (ps) under strongly superheated conditions in agreement with MD simulations performed on nanostructures.<sup>8,10,11</sup> Finally, we image the re-solidification dynamics and compare our results with the re-solidification dynamics of initially smooth surfaces.

## RESULTS AND DISCUSSION

### Ultrafast ultramicroscopy on surface nanostructures

The experimental setup is shown in [Figure 1A](#) (see [Supplemental experimental procedures](#)). Briefly, an ultramicroscope is a dark-field imaging device that suppresses background reflection by collecting scattered light only through proper positioning of the objective lens. In our case, the pump and probe beams are incident on the sample surface at 36 and 18°, respectively, while the imaging optics is positioned normal to the sample surface. Amplified Ti:sapphire laser generates 65 fs with a central wavelength of 800 nm. The pump and probe beams are produced by a beam splitter, and the probe beam is directed to a BBO crystal that generates second harmonic radiation with a wavelength of 400 nm. We use a variable optical delay line with a delay time range between 100 fs and 408 ns. An electromechanical shutter controls the number of pulses and is set to pass single pump and probe pulses. Finally, scattered light from the pump is blocked using a blue short-pass filter. Our experimental setup is suitable for determining the characteristic phase-transformation timescales as it spans the femto-, pico-, and nanosecond (ns) ranges.

Our ultramicroscope can image nanostructures via a single shot of non-destructive optical probe beam (see [Figures S1–S5](#)). The concept of ultramicroscope imaging

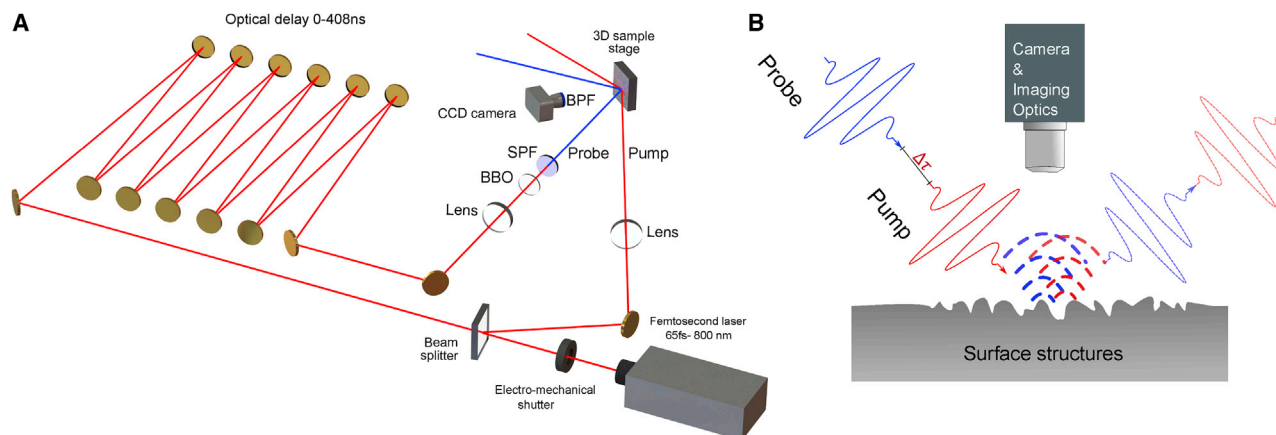


**Figure 1. Ultrafast ultramicroscopy of surface nanostructures**

(A and B) A schematic of (A) ultrafast ultramicroscope setup and (B) ultrafast ultramicroscopy's working principle. See also [Figures S1–S5](#).

of surface nanostructures is shown in [Figure 1B](#). A pump pulse is incident on nano-scale surface structures followed by a delayed probe pulse with a delay time  $\Delta\tau$ . Photo-induced phase transitions that obscure the scattered light appear as a dark spot. By comparing the transient image with the initial image, i.e., before the pump, we obtain information on the phase transition of the nanostructure. Furthermore, by comparing the transient image with the final image, we can determine when re-solidification takes place. We study the photo-induced phase transition dynamics of Zn surface nanostructures. The structures are formed by ablating a polished Zn substrate with a laser fluence of  $F = 1.0 \text{ J/cm}^2$ , leading to nanostructures covering the Zn surface with an average diameter of  $\sim 153 \pm 111 \text{ nm}$ .

[Figures 2A–2D](#) present time-series snapshots of the Zn surface nanostructures as they undergo photo-induced phase transition following a pump laser fluence  $F = 1.0 \text{ J/cm}^2$  (for full time-series images, see [Figures S6](#) and [S7](#)). We compare the ultramicroscope image of the initial surface nanostructures with the transient surface image obtained after the pump at a given delay time  $\Delta\tau$ . For each preset delay, the samples were laterally shifted to get a polished “fresh” surface. The fresh surface is then irradiated with a single laser pulse to create surface structures. Afterward, we perform the pump-probe imaging procedure.

We compare the initial and transient images for each delay time (see [Note S1](#)). At  $\Delta\tau = 0 \text{ ps}$ , the images are nearly identical ([Figure 2A](#)) as expected. However, at  $\Delta\tau = 6 \text{ ps}$ , the scattering from parts of the surface ([Figure 2B](#), left) has disappeared ([Figure 2B](#), right). The scattering signal disappearance disseminate across the sample as  $\Delta\tau$  increases, indicating the spread of melting and ablation of surface structures as shown for  $\Delta\tau = 10$  and  $283 \text{ ps}$  ([Figures 2C](#) and [2D](#)). [Figure 2E](#) presents the image comparison analysis performed by comparing the transient and initial images that provides an objective characterization of the obtained images. Clearly, the similarity decreases within a few ps, and almost no similarity exists after hundreds of ps.

### Photomechanical spallation from nanostructures

We note that melting of nanostructures cannot explain the suppression of scattered light. [Figures 3A](#) and [3B](#) show FDTD calculation of scattering from a  $150 \text{ nm}$  Zn sphere (see [Note S3](#)). While liquid Zn has lower scattering than solid Zn,<sup>18</sup> the difference is negligible and cannot explain the suppression of the scattering signal

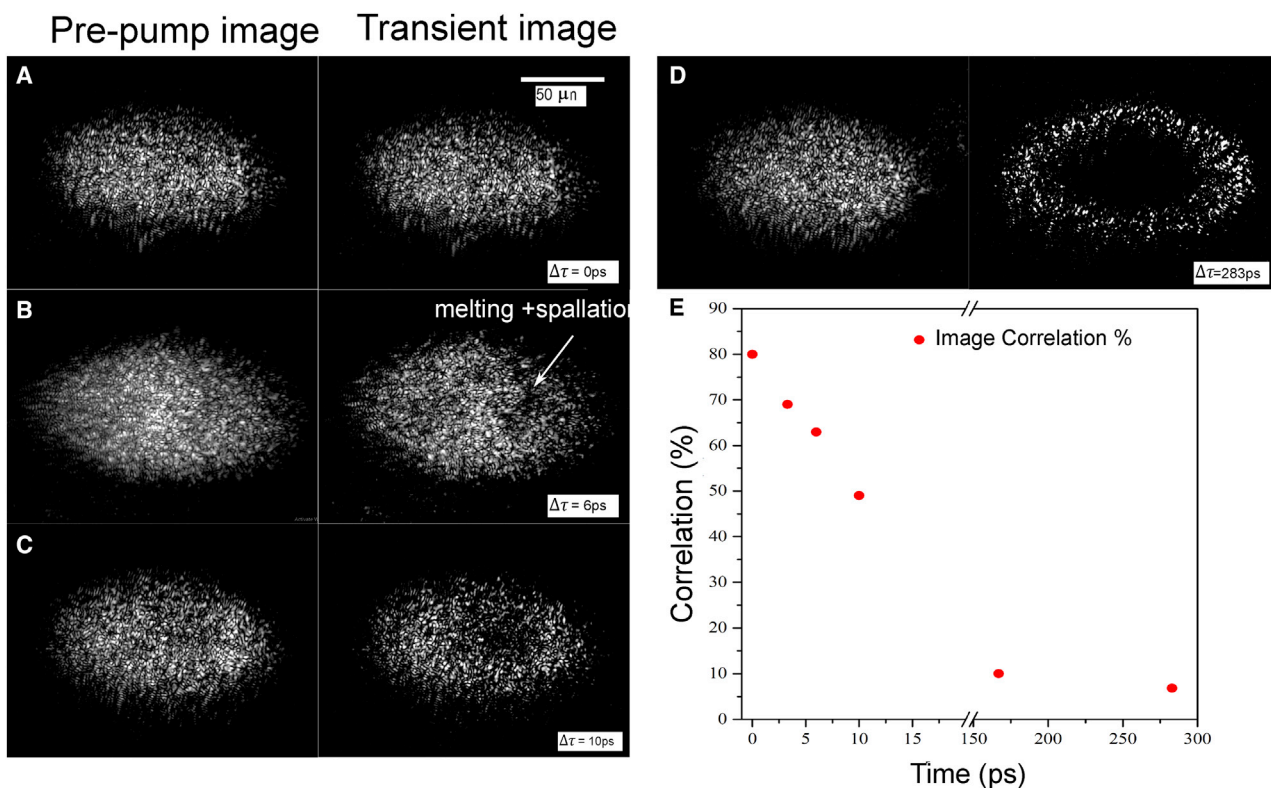


**Figure 2. Imaging the photo-induced phase transition of Zn surface structures**

(A–D) Single-shot image of surface structures formed on Zn surface before (left) and after (right) exciting the surface with a pump pulse fluence  $F = 1.0\text{ J/cm}^2$  at (A)  $\Delta\tau = 0\text{ ps}$ , (B)  $\Delta\tau = 6\text{ ps}$ , (C)  $\Delta\tau = 10\text{ ps}$ , and (D)  $\Delta\tau = 283\text{ ps}$ . Scale bar, 50  $\mu\text{m}$ .

(E) Image comparison analysis that determines the correlation between the initial image with the transient image. See also [Figures S6 and S7](#).

observed in our experiments. For scattering to be fully suppressed either the surface topology must be smooth, or the scattering cross section of the surface structures drops significantly.

We show here that scattering suppression is due to spallation of surface nanostructures, as predicted by MD simulations,<sup>8,10,11</sup> which enjoy weaker scattering and higher absorption. The normalized scattering and absorption cross sections of an individual Zn nanoparticle versus  $D$  are shown in [Figure 3D](#), inset. Because of the  $D^6$  dependence of scattering, individual spalled structures with  $D = 3\text{ nm}$  have 8 decades lower scattering than the original particle with  $D = 150\text{ nm}$ . The calculated total scattering and absorption of  $N$  particles with a volume equal to that of a 150 nm sphere for different particle diameters are shown in [Figure 3D](#). The latter calculation considers the case where a 150 nm nanoparticle is spalled into smaller particles with a given diameter. Note that the  $D^6$  dependence applies only to the calculated scattering and absorption of individual nanoparticles and is valid for particle sizes where the quasi-static approximation applies.<sup>19</sup> The total absorption increases by over two decades, while the total scattering decreases by over two decades, as  $D < 20\text{ nm}$ . Therefore, the absorption will dominate scattering for a cloud of particles with  $D < 20\text{ nm}$ . Accordingly, the sudden decrease in scattering signal is due to spallation of a surface structure into particles with  $D < 20\text{ nm}$ , which is in general agreement with MD simulations on nanoparticles. Note that even if the surface below the spalled structures is inhomogeneous, it would be shadowed by the spalled highly absorbing objects. Our observations indicate that spallation of existing

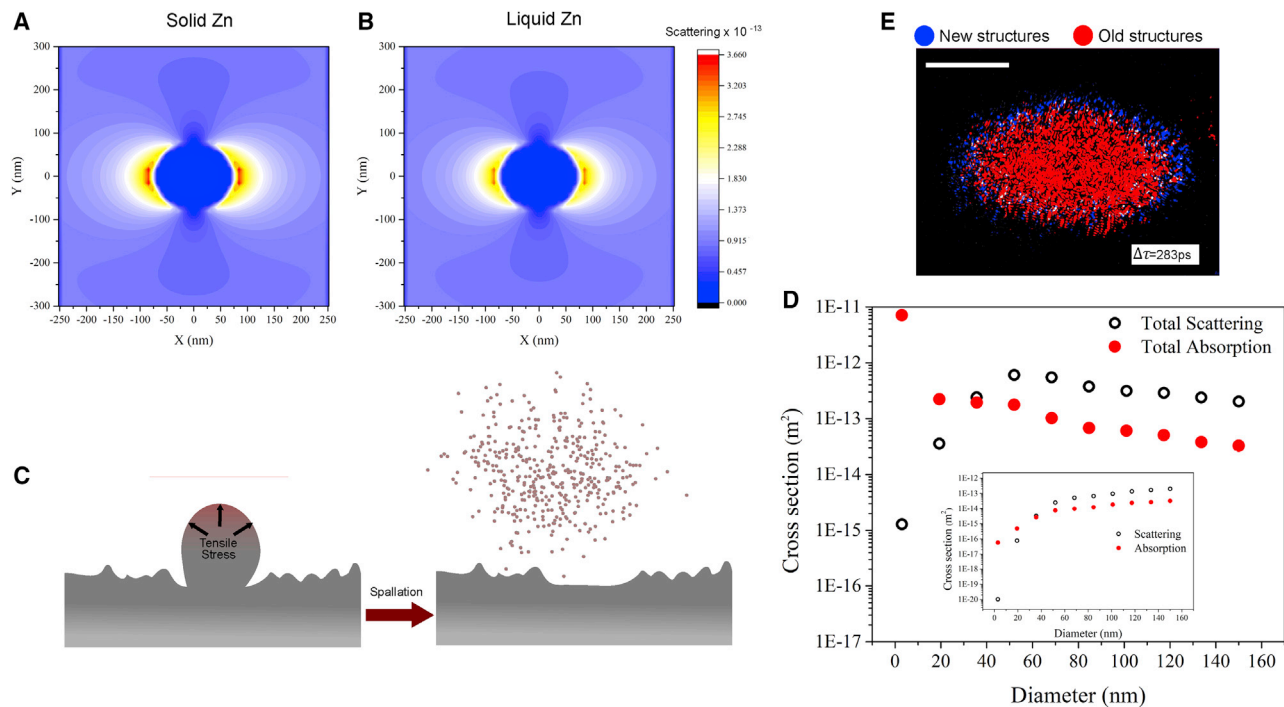


**Figure 3. Origin of scattering suppression**

(A and B) FDTD calculation of scattering from a 150 nm (A) solid Zn sphere and (B) liquid Zn sphere.

(C) Schematics of photomechanical spallation process in surface nanostructures.

(D) Calculated scattering and absorption versus diameter of  $N$  Zn particles with the same volume as a 150 nm Zn sphere. Inset: calculated scattering and absorption of individual Zn nanospheres as a function of the sphere's diameter.

(E) Image correlation analysis that compares the initial and transient Zn surface structures at  $\Delta\tau = 283$  ps. The erased structures are shown in red color and newly formed structures in blue color. The nascent structures form at the periphery of the original structures.

nanostructures occurs initially at random sites and expands away from the sites for a few hundred picoseconds. The observed inhomogeneous spallation across the substrate is likely due to the initial spatial inhomogeneity of surface structures, which can lead to inhomogeneous absorption of the incident laser pulse at the nanoscale, i.e., the lightning rod effect.

We also observed the formation of nascent structures at the periphery of the original surface structures. Nascent structures can appear due to various mechanisms, e.g., Marangoni effect, hydrodynamic motion due to pressure relaxation, and re-deposition of spalled or ablated particles.<sup>20</sup> Figure 3E shows surface structures with faux colors representing the old structures in red and nascent structures in blue by comparing the images obtained in Figure 2D ( $\Delta\tau = 283$  ps) (see Figures S8 and S9). The formation of nascent surface inhomogeneities can be explained based on various mechanisms. At the sub-nanosecond timescale, surface fluctuations are more likely to occur due to pressure relaxation in the melted layer. Pressure relaxation creates hydrodynamic motion-induced surface fluctuations where the fluctuations are governed by the speed of sound in the melted materials. From our images, we can see that nascent structures exist at a fresh surface  $\sim 1$   $\mu\text{m}$  away from original structures.<sup>17</sup> The estimated  $\tau^{\text{nascent}} \sim 450$  ps based on pressure relaxation agrees with our observation of  $\tau^{\text{nascent}} \sim 200 - 300$  ps (see Note S4). Importantly, this observation consolidates our argument that spallation of existing structures suppresses scattering where the structures initially existed, i.e., only scattering from regions where no initial structures exist is observed.

### Re-solidification dynamics of surface nanostructures

Finally, as the lattice heat dissipates, solidification starts and transient structures begin to resemble the final structure. The re-solidification process of bulk materials is expected to extend to 10s - 100s nanoseconds and to depend on the total energy absorbed by the substrate and the heat diffusion properties of the substrate.<sup>8,9</sup> The solidification time of surface structures can be calculated by considering thermal conduction as the main cooling mechanism for ultrafast laser heating.  $\tau^{solid}$  depends on the spatial scale of the temperature field  $z$  and the thermal diffusivity  $\chi$ , which given by previous work:<sup>17,21</sup>

$$\tau^{solid} = z^2 / 4\chi, \quad z \equiv \left( \frac{18 I_A k}{g^2 T_0} \right)^{1/3} \quad (\text{Equation 1})$$

where  $I_A$  is the absorbed intensity,  $T_0$  is the ambient temperature,  $g$  is the electron-phonon coupling factor, and  $k$  is the thermal conductivity. The estimated  $\tau^{solid}$  from Equation 1 is 200 and 37 ns for  $F = 1 \text{ J/cm}^2$  and  $F = 0.1 \text{ J/cm}^2$ , respectively.

To experimentally study the re-solidification of nanostructures, we compare the transient images obtained at a given delay time  $\Delta\tau$  and the final structures formed due to  $P$  at  $\Delta\tau = \infty$  via the frame-reference method.<sup>16</sup> As shown in Figures 4A–4C, nascent surface structures form and repopulate the entire irradiated region. By comparing the transient and final images, we can determine the re-solidification time for the entire structure, which appears to be in the order of 100 ns (see Figures S10–S12). Similarly, Figures 4D and 4F compare the ultramicroscope images of surface structures irradiated with laser fluence  $F = 0.1 \text{ J/cm}^2$ . The transient structures start resembling final structures even within few hundreds of ps as shown in Figures 4E and 4F. The transient and final structures are very similar at  $\Delta\tau = 527 \text{ ps}$  and are nearly identical at  $\Delta\tau = 2.8 \text{ ns}$ . Furthermore, it was experimentally shown that  $\tau^{solid}$  of bulk Zn ablated with  $F = 0.1 \text{ J/cm}^2$  is approximately 124 ns, i.e., at least a decade longer than  $\tau^{solid}$  for nanostructured Zn surface as in our study.<sup>17</sup> Our results confirm MD simulations that showed that spallation leads to a reduction in the duration of the re-solidification process.<sup>8,9</sup>

Note that plasma generation does not seem to play a dominant role in explaining the observed suppression of scattered light. Plasma was shown to initially generate homogeneously across the laser-irradiated region below 1 ps.<sup>22,23</sup> Even assuming that micro-plasmas are generated from nanostructures and microstructures, the scattered signal would disappear below 1 ps. Moreover, early-stage plasma expansion from fs laser ablation expands primarily perpendicular to the ablated surface. After several nanoseconds, the plasma expands in lateral and perpendicular directions.<sup>21,24</sup> Our images show rapid (picosecond) lateral expansion of the “dark” spot, which does not support the dynamics of micro-plasmas expansion. Finally, the lifetime of the generated plasma lasts up to 1,000 s of nanoseconds. Consequently, if the plasma plume had any contribution, we would not have observed the re-solidification of surface structures within few tens of nanoseconds.

Since scattering is a universal property, our technique is not limited by the type of material used.<sup>9</sup> Because of its simplicity, ultrafast ultramicroscopy will be valuable for the study of photo-induced phase transitions. Our method can image processes that require higher temporal resolution than that of existing electron-beam pulses, e.g., non-thermal melting. The diffraction limited spatial resolution did not limit our ability to image nanoscale dynamics. Future works can enhance the resolution using tunable probe wavelengths,<sup>25</sup> using algorithms to enhance the imaging resolutions, or using image processing neural networks.<sup>26,27</sup>

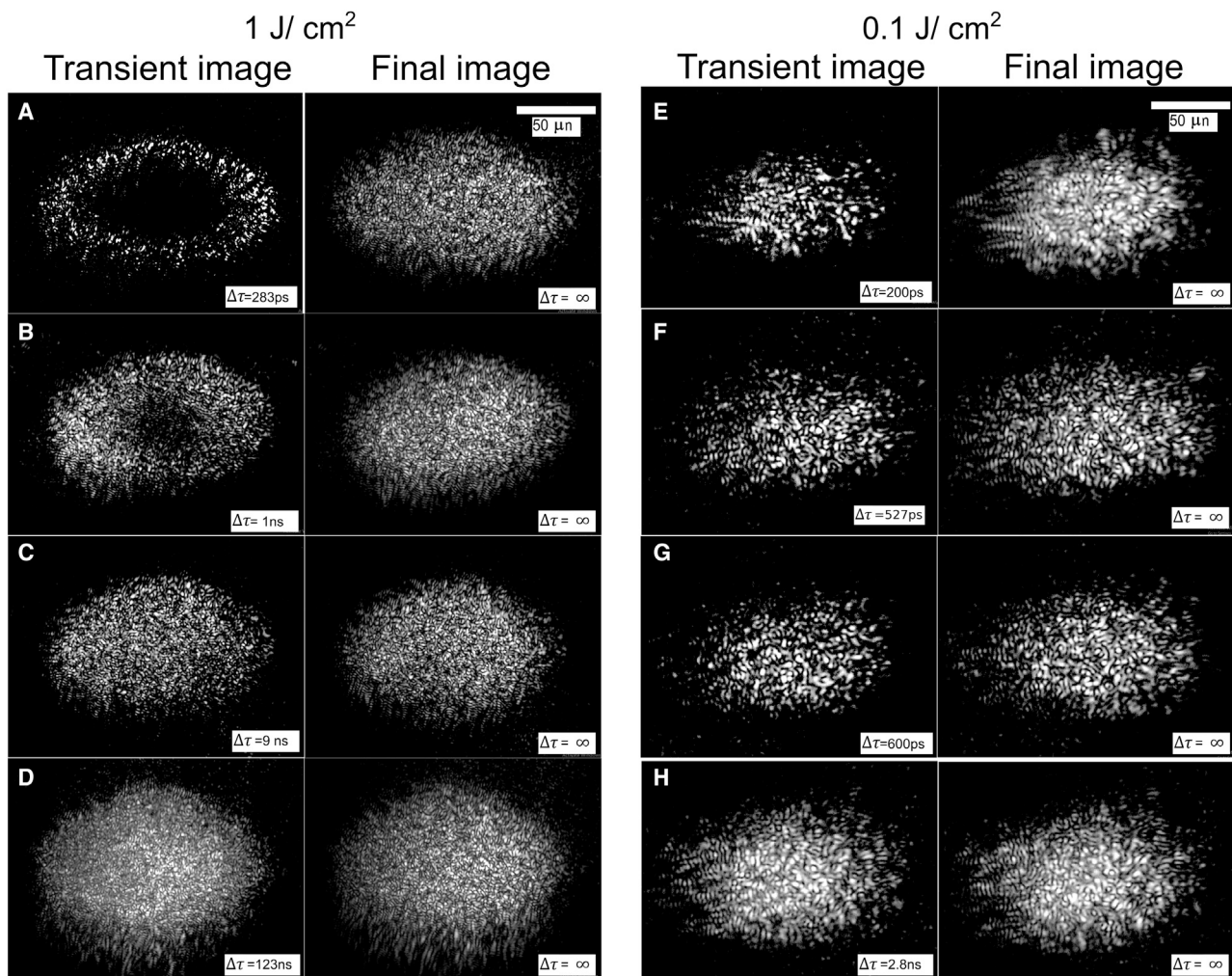


**Figure 4. Imaging the solidification dynamics of Zn surface structures**

(A–C) Compare the transient structures (left) versus final (right) structures formed after irradiation with  $F = 1.0 \text{ J/cm}^2$  pump pulse at (A)  $\Delta\tau = 283 \text{ ps}$ , (B)  $\Delta\tau = 1 \text{ ns}$ , and (C)  $\Delta\tau = 123 \text{ ns}$ .

(D–F) Compare the transient structures (left) versus final (right) structures formed after irradiation with  $F = 0.1 \text{ J/cm}^2$  pump pulse at (D)  $\Delta\tau = 200 \text{ ps}$ , (E)  $\Delta\tau = 527 \text{ ps}$ , and (F)  $\Delta\tau = 2.8 \text{ ns}$ . Scale bar,  $50 \mu\text{m}$ . See also Figures S10–S12.

To conclude, we showed that ultrafast laser irradiation provides a unique tool for preparing and studying extreme states of condensed matter at the nanoscale with widely existing experimental tools. Using a variety of numerical tools, we correlated the optical properties of the surface nanostructures with photo-induced phase transitions. We optically imaged the melting and spallation of nanoscale structures, as opposed to what was studied previously using electron-beam diffraction that relied on tracking the loss of long-range lattice order to infer its existence.<sup>28,29</sup> Our results agree with MD simulations on nanoparticles. We showed that the solidification time is an order of magnitude shorter for nanostructures surfaces compared with unstructured surfaces.

## EXPERIMENTAL PROCEDURES

### Resource availability

#### Lead contact

Further information and requests for resources should be directed to, and will be fulfilled by, the lead contact, Prof. Chunlei Guo ([guo@optics.rochester.edu](mailto:guo@optics.rochester.edu)).

### Materials availability

This study did not generate new unique reagents.

### Data and code availability

All the data associated with this study are included in the article and in the [Supplemental information](#). Additional information is available from the lead contact upon reasonable request.

## SUPPLEMENTAL INFORMATION

Supplemental information can be found online at <https://doi.org/10.1016/j.xcrp.2021.100651>.

## ACKNOWLEDGMENTS

We acknowledge the fruitful discussions with L. Zhigilei. We acknowledge the support of the Army Research Office and Bill & Melinda Gates Foundation.

## AUTHOR CONTRIBUTIONS

A.Y.V. and C.G. discussed and defined the project. R.F., M.E., A.Y.V., and S.A.J. performed the experiments. R.F. and A.Y.V. developed the original setup. M.E. and S.C. performed the FDTD calculations. M.E. analyzed the data. B.L. and S.C.S. provided experimental supports. M.E. and C.G. wrote the manuscript with feedback from all the authors.

## DECLARATION OF INTERESTS

C.G. is a board member of *Cell Reports Physical Science*.

Received: June 13, 2021

Revised: September 9, 2021

Accepted: October 27, 2021

Published: November 18, 2021

## REFERENCES

- Vorobyev, A., and Guo, C. (2009). Metal pumps liquid uphill. *Appl. Phys. Lett.* *94*, 224102.
- Vorobyev, A.Y., and Guo, C. (2013). Direct femtosecond laser surface nano/microstructuring and its applications. *Laser Photonics Rev.* *7*, 385–407.
- Zhan, Z., ElKabbash, M., Cheng, J., Zhang, J., Singh, S., and Guo, C. (2019). Highly Floatable Superhydrophobic Metallic Assembly for Aquatic Applications. *ACS Appl. Mater. Interfaces* *11*, 48512–48517.
- Sher, M.-J., Hammond, K., Christakis, L., and Mazur, E. (2013). The photovoltaic potential of femtosecond-laser textured amorphous silicon (International Society for Optics and Photonics), p. 86080R.
- Zhang, J., ElKabbash, M., Wei, R., Singh, S.C., Lam, B., and Guo, C. (2019). Plasmonic metasurfaces with 42.3% transmission efficiency in the visible. *Light Sci. Appl.* *8*, 53.
- Singh, S.C., ElKabbash, M., Li, Z., Li, X., Regmi, B., Madsen, M., Jalil, S.A., Zhan, Z., Zhang, J., and Guo, C. (2020). Solar-trackable superwicking black metal panel for photothermal water sanitation. *Nat. Sustain* *3*, 938–946.
- Vorobyev, A.Y., and Guo, C. (2006). Femtosecond laser nanostructuring of metals. *Opt. Express* *14*, 2164–2169.
- Zhigilei, L.V., Lin, Z., and Ivanov, D.S. (2009). Atomistic Modeling of Short Pulse Laser Ablation of Metals: Connections between Melting, Spallation, and Phase Explosion. *J. Phys. Chem. C* *113*, 11892–11906.
- Zhigilei, L.V., Lin, Z., Ivanov, D.S., Leveugle, E., Duff, W.H., Thomas, D., Sevilla, C., and Guy, S.J. (2010). Atomic/Molecular-Level Simulations of Laser–Materials Interactions. In *Laser-Surface Interactions for New Materials Production: Tailoring Structure and Properties*, A. Miotello and P.M. Ossi, eds. (Springer), pp. 43–79.
- Fahdiran, R., and Urbassek, H.M. (2015). *Laser Ablation of Nanoparticles: A Molecular Dynamics Study* (Trans Tech Publications), pp. 120–123.
- Fahdiran, R., Handoko, E., Sugihartono, I., and Urbassek, H.M. (2018). Laser induced ablation of aluminum nanoparticle: a molecular dynamics study (EDP Sciences), p. 04004.
- Barty, A., Boutet, S., Bogan, M.J., Hau-Riege, S., Marchesini, S., Sokolowski-Tinten, K., Stojanovic, N., Tobey, R.a., Ehrke, H., Cavalleri, A., et al. (2008). Ultrafast single-shot diffraction imaging of nanoscale dynamics. *Nat. Photonics* *2*, 415.
- Spence, J. (2008). Ultrafast diffract-and-destroy movies. *Nat. Photonics* *2*, 390.
- Barwick, B., and Zewail, A.H. (2015). Photonics and Plasmonics in 4D Ultrafast Electron Microscopy. *ACS Photonics* *2*, 1391–1402.
- Zewail, A.H. (2010). Four-dimensional electron microscopy. *Science* *328*, 187–193.
- Hassan, M.T. (2018). Attomicroscopy: from femtosecond to attosecond electron microscopy. *J. Phys. At. Mol. Opt. Phys.* *51*, 032005.
- Fang, R.R., Vorobyev, A., and Guo, C.L. (2017). Direct visualization of the complete evolution of femtosecond laser-induced surface structural dynamics of metals. *Light Sci. Appl.* *6*, ARTN e16256.
- Siegel, E. (1976). Optical reflectivity of liquid metals at their melting temperatures. *Phys. Chem. Liquids* *5*, 9–27.

19. Fan, X., Zheng, W., and Singh, D.J. (2014). Light scattering and surface plasmons on small spherical particles. *Light Sci. Appl.* 3, e179, e179.
20. Rosenfeld, A., Höhm, S., Krüger, J., and Bonse, J. (2017). Dynamics of ultrashort double-pulse laser ablation of solid surfaces. In *Reference Module in Chemistry, Molecular Sciences and Chemical Engineering, Encyclopedia of Interfacial Chemistry: Surface Science and Electrochemistry*, J. Reedijk, ed. (Elsevier), pp. 1–10.
21. Agranat, M.B., Ashitkov, S.I., Fortov, V.E., Kirillin, A.V., Kostanovskii, A.V., Anisimov, S.I., and Kondratenko, P.S. (1999). Use of optical anisotropy for study of ultrafast phase transformations at solid surfaces. *Appl. Phys., A Mater. Sci. Process.* 69, 637–640.
22. Nishikino, M., Hasegawa, N., Tomita, T., Minami, Y., Eyama, T., Kakimoto, N., Izutsu, R., Baba, M., Kawachi, T., and Suemoto, T. (2017). Formation of x-ray Newton's rings from nano-scale spallation shells of metals in laser ablation. *AIP Adv.* 7, 015311.
23. Sokolowski-Tinten, K., Bialkowski, J., Cavalleri, A., von der Linde, D., Oparin, A., Meyer-ter-Vehn, J., and Anisimov, S.I. (1998). Transient States of Matter during Short Pulse Laser Ablation. *Phys. Rev. Lett.* 81, 224–227.
24. Anisimov, S.I., and Rethfeld, B. (1997). Theory of ultrashort laser pulse interaction with a metal (SPIE).
25. Bonse, J. (2017). Scattering on scattering. *Light Sci. Appl.* 6, e17088.
26. Wang, H., Rivenson, Y., Jin, Y., Wei, Z., Gao, R., Günaydin, H., Bentolila, L.A., Kural, C., and Ozcan, A. (2019). Deep learning enables cross-modality super-resolution in fluorescence microscopy. *Nat. Methods* 16, 103–110.
27. Barbastathis, G., Ozcan, A., and Situ, G. (2019). On the use of deep learning for computational imaging. *Optica* 6, 921–943.
28. Mo, M.Z., Chen, Z., Li, R.K., Dunning, M., Witte, B.B.L., Baldwin, J.K., Fletcher, L.B., Kim, J.B., Ng, A., Redmer, R., et al. (2018). Heterogeneous to homogeneous melting transition visualized with ultrafast electron diffraction. *Science* 360, 1451–1455.
29. Siwick, B.J., Dwyer, J.R., Jordan, R.E., and Miller, R.J.D. (2003). An atomic-level view of melting using femtosecond electron diffraction. *Science* 302, 1382–1385.